Journal of Nuclear Materials 389 (2009) 450–457

Contents lists available at ScienceDirect

Journal of Nuclear Materials

journal homepage: www.elsevier.com/locate/jnucmat

Behaviour of ruthenium dioxide particles in borosilicate glasses and melts

Rachel Pflieger [a,b,*], Leila Lefebvre [a], Mohammed Malki [c,d], Mathieu Allix [c], Agnès Grandjean [a,b]

[a] DEN/DTCD-SCDV/CEA Valrhô, Centre de Marcoule, BP17171, 30207 Bagnols-sur-Cèze, France
[b] Institut de Chimie Séparative de Marcoule, UMR5257, Centre de Marcoule, BP17171, 30207 Bagnols-sur-Cèze Cedex, France
[c] CNRS/CEMHTI-1D Av. de la Recherche Scientifique, 45701 Orléans cedex 2, France
[d] Polytech' Orleans, Université d'Orléans, 8 rue Léonard de Vinci, 45072 Orléans cedex 2, France

ARTICLE INFO

Article history:
Received 28 September 2008
Accepted 23 February 2009

ABSTRACT

Ruthenium–glass systems are formed during the vitrification of nuclear waste. They are also widely used in micro-electronics because of their unique electrical properties. However, the interaction of this element with the glass matrix remains poorly understood. This work focuses on a RuO_2 particles-nuclear alumino-borosilicate glass system in which the electrical conductivity is known to vary considerably with the RuO_2 content and to become electronic above about 0.5–0.7 vol.% RuO_2 [R. Pflieger, M. Malki, Y. Guari, J. Larionova, A. Grandjean, J. Am. Ceram. Soc., accepted for publication]. Some RuO_2 segregation was observed in SEM/TEM investigations but no continuous chain of RuO_2 particles could be seen. Electron relays between the particles are then necessary for a low-rate percolation, such as the nanoclusters suggested by Adachi et al. [K. Adachi, S. Iida, K. Hayashi, J. Mater. Res. 9 (7) (1994) 1866; K. Adachi, H. Kuno, J. Am. Ceram. Soc. 83 (10) (2000) 2441], which could consist in dissolved ruthenium. Indeed, several observations made here clearly indicate the presence of dissolved ruthenium in the glass matrix, like the modification of the glass density in presence of RuO_2 particles or the diffusion-limited growth of RuO_2 particles in the melt.

1. Introduction

The fission product ruthenium is a peculiar component of spent nuclear fuel. Although its amount is low (around a few percents), its complex chemistry is of great importance in the process of immobilisation of nuclear waste within glass. Its solubility in glass is very low (some tens to some thousands of parts per million [4,5]) and most of the ruthenium in glass can be found in the form of RuO_2 precipitates.

Ruthenium shows a particular behaviour in comparison with the other platinum group metals, which results in a modification of several macroscopic properties of the glass. For example, the particular interaction between ruthenium dioxide and the glass matrix makes RuO_2–glass composites materials with unique electrical properties: at very low ruthenium contents (a few vol.%) an electronic contribution to the conductivity appears [6] and the resistivity varies over several orders of magnitude with RuO_2 content [7]. This is why such composites have been widely used in electronic applications such as thick film resistors (see for example [8] and [2]). The electrical conductivity of the glass melt is also a key parameter in the process of nuclear waste vitrification, the waste-glass frit mixture being heated by Joule effect, and the electrical conductivity of RuO_2–glass frit composites has been studied in our laboratories both in the solid and molten states [1,9], showing a percolation threshold below 1 vol.%, so far below the RuO_2 amount necessary for a geometrical percolation (i.e., necessary for randomly distributed spheres to touch), which is 16 vol.% [10] but in good agreement with the results obtained on lead glasses by Kusy [11] in the 4.2–300 K temperature range (v_c = 2–4 vol.%). This very low percolation threshold might be partially explained by a connected network formed by the RuO_2 particles but since the particles are always separated by a glass film, 'relays' for the electrons are necessary, such as nanoparticles of Ru or RuO_2, or dissolved ruthenium atoms/ions. This role of dissolved ruthenium as tunnelling resonant centres was suggested by Pike and Seager in [12]. However, this theory has not been proved yet.

Another physical property extensively modified by the presence of ruthenium dioxide is the viscosity of the glass melt that increases with RuO_2 content, even at low contents (about 1 wt% i.e. 0.3 vol.%; see e.g. [13]). These modifications of several properties of the glass matrix are the signs of a strong interaction between ruthenium dioxide and the glass matrix, which needs to be investigated in more details.

Though ruthenium in glass is mostly in the form of RuO_2 precipitates, its volatility is not negligible at temperatures above 1000 °C. Since ruthenium is a fission product, its volatility has been studied in the context of the dissolution of spent nuclear fuel in nitric acid

* Corresponding author. Present address: Institut de Chimie Séparative de Marcoule, UMR5257, Department of Sonochemistry, Centre de Marcoule, BP17171, 30207 Bagnols-sur-Cèze Cedex, France. Tel.: +33 (0) 4 66 33 92 50; fax: +33 (0) 4 66 79 76 11.
E-mail addresses: rachel_pflieger@yahoo.fr, rachel.pflieger@cea.fr (R. Pflieger).

0022-3115/$ - see front matter © 2009 Elsevier B.V. All rights reserved.
doi:10.1016/j.jnucmat.2009.02.034

[14,15] and of nuclear power plant severe accidents (for a recent review see [16]). In particular it has been shown that the vapour of ruthenium dioxide in air contains significant amounts of RuO_3 and RuO_4 (e.g., under thermodynamic equilibrium at 1100 °C and 1 bar pressure: 2 wt% RuO_3 and 0.2 wt% RuO_4 [17]). On the other hand, only little literature exists on ruthenium volatilisation from glasses. Kamizono et al. [18] studied ^{106}Ru concentration in a closed stainless-steel canister containing high-level waste in a borosilicate glass by a γ-radiation scanning method. They found the equilibration time to be quite long, in the order of 24 h at 600 °C, and observed some reaction of the vapour with the stainless-steel walls, leading to reprecipitation of RuO_2. Another important report on the volatilisation of ruthenium from borosilicate glass melts is the one of Wilds [19]. This author submitted borosilicate glasses containing 0.05 or 0.15 wt% RuO_2 to a 3-h-thermal treatment at 1150 °C. He observed that between 2.8 and 7.5 wt% of the ruthenium was volatilised, depending on the composition of the glass (high Al- or high Fe-rate) and on the atmosphere (Ar or air).

In this paper, we focus our attention on the interaction of RuO_2 with one particular borosilicate glass, the composition of which is very close to the one of the glass frit used in France for the vitrification of nuclear waste. Ruthenium volatility from this glass is measured and the influence of the glass on this volatility is discussed. We then try to bring to light how RuO_2 modifies the glass density. The interaction between ruthenium dioxide and the glass is also demonstrated by the growth of RuO_2 crystallites in the glass melt, which was followed by X-ray diffraction.

2. Experimental procedure

2.1. Sample preparation

Studied samples were composites of RuO_2 particles and glass frit FNOC57, the glass frit usually used for the confinement of French nuclear waste. The composition of this glass frit is given in Table 1. Samples were prepared by mixing powders of glass frit and of RuO_2 (HERAEUS), grinding them together in an agate mortar, melting the mixture placed in an alumina crucible at temperatures between 1000 and 1500 °C and heating for two hours. Various RuO_2 contents were studied for each synthesis temperature, in the range 0–4 wt% (a sample containing 8 wt% RuO_2 was also prepared at 1100 °C). The densities of FNOC57 and RuO_2 are 2.49 and 6.97 g cm^{-3}, respectively, and the glass transition temperature of FNOC57 is about 520 °C. A series of composites was also synthesised using an acidic solution of ruthenium nitrosyle nitrate as RuO_2 precursor: the mixture of the powdered glass frit and solution, placed in an alumina crucible, was first dried at 120 °C for 20 h; it was then submitted to a 2-h-heat treatment in a muffle furnace.

Obtained composites were quenched in air and then annealed at about 20 °C below their glass transition temperature (i.e., at 500 °C) for 12 h followed by a slow cooling down to room temperature.

Table 1
Measured composition of the glass frit FNOC57.

	FNOC57, wt%
Al_2O_3	4.28
B_2O_3	18.15
CaO	5.23
Li_2O	2.56
Na_2O	7.00
SiO_2	58.84
ZnO	3.24
ZrO_2	0.70

Volatility measurements were also performed on a series of sodium borosilicate glasses (SiO_2–B_2O_3–Na_2O glasses) with a fixed SiO_2/B_2O_3 mass ratio (equal to 1.83) and Na_2O contents of 12, 15, 20, 25 and 30 wt%. These glasses (called SBN_x, with x the initial mass fraction of Na_2O) were prepared as described in [20]. The obtained quenched glasses were then grinded, and for each composition two 17.5 g samples were prepared in alumina crucibles and submitted to the same heat treatment (3 h at 1200 °C followed by a quenching in air): a reference one of the pure SBN_x glass, and one in which the SBN_x powder was mixed to 4 wt% RuO_2 powder.

2.2. Density measurements

Densities were measured on monolithic annealed samples using a hydrostatic balance based on Archimedes' principle. For each composition, density measurements were performed either once on six glass pieces or three times on one glass piece, and the mean value was calculated. The accuracy was estimated to be about 2×10^{-3} g cm^{-3}.

2.3. Volatility of RuO_2

The knowledge of ruthenium oxide volatility during heat treatments of RuO_2–glass composites at temperatures above 1000 °C is necessary for the estimation of RuO_2 amounts in studied samples. In order to determine this volatility, samples were systematically weighed before and after each heat treatment. This fast and simple method was chosen because it presents the advantage of avoiding sampling in non-always homogeneous samples. The obtained mass losses Δm were then compared to the mass loss Δm_{frit} of the corresponding reference sample, namely pure glass frit FNOC57 submitted to the same heat treatment. Subsequently, the mass fraction of RuO_2 lost by evaporation was obtained from the following formula, where m_{RuO_2} is the RuO_2 mass introduced in the sample:

$$x_{RuO_2}^{vap} = \frac{\Delta m - \Delta m_{frit}}{m_{RuO_2}} \quad (1)$$

The ratio of the free evaporating (geometric) surface to the mixture powder mass was kept constant and equal to 0.266 or 0.229 cm^2/g (±5%), depending on the experiment series. No significant difference was observed in the volatilities observed with both ratios.

For comparison, similar volatility measurements were also performed on pure RuO_2 samples submitted to a 2-h heat treatment (at 900, 1100 or 1300 °C) under an argon flux.

2.4. Electron microscopies

The FNOC57–RuO_2 samples containing 4 wt% RuO_2 were also studied by scanning electron microscopy (SEM) and by transmission electron microscopy (TEM). SEM measurements were performed on carbon-coated polished samples, using a JEOL 6330F field-emission microscope. For TEM investigations, samples were first crushed in ethanol, and the small glass particles in suspension were deposited onto a holey carbon film, supported by a copper grid. The electron diffraction and imaging were carried out with a PHILIPS CM20 microscope operating at 200 kV and equipped with an OXFORD analyser which allowed us to localise ruthenium.

2.5. XRD spectra

Studied glasses were first ground to fine powder in an agate mortar. The diffraction data were collected at room temperature

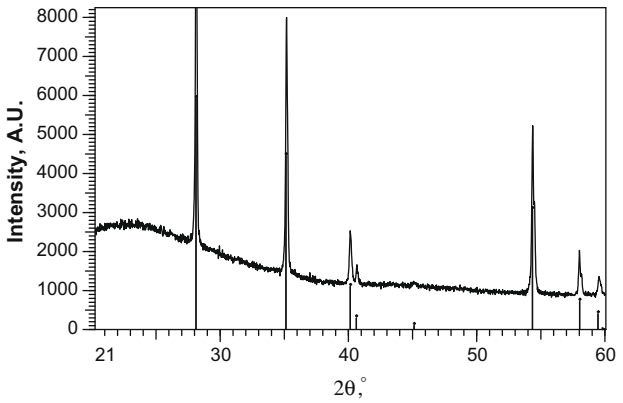

Fig. 1. Raw room temperature diffractogram of a FNOC57–4 wt% RuO_2 composite synthesized at 1300 °C. Indexation lines correspond to the RuO_2 reference (JCPDS sheet 00-040-1290).

using a Bragg Brentano diffractometer in the θ/θ geometry, with a Cu anticathode ($\lambda(K_{\alpha 1}) = 1.54060$ Å, $\lambda(K_{\alpha 2}) = 1.54439$ Å, 40 kV, 20 mA) and a linear detector. The angular range $2\theta = 10$–$110°$ was scanned at 1.2° min^{-1} using 0.0174° steps. Composites with 4 wt% RuO_2 were also synthesised *in situ*, by heating the mixed powder of FNOC57 + 4 wt% RuO_2 placed on a Pt pellet in the diffractometer; a fast temperature ramp (1600 °C/min) up to 900, 1050, 1100 or 1200 °C was used, followed by a temperature plateau of several hours. Successive scans within the $2\theta = 26.5$–$29.0°$ (steps of 0.0174°, counting time per step of 1.2 s) range were then performed during this plateau, and in the end at room temperature, after a fast temperature decreasing ramp of approximately 2–3 min (ramp of 400 °C/min). A typical raw diffractogram is shown in Fig. 1.

Obtained diffractograms were treated using the WINPLOTR software: they were corrected for background, the relative contribution of $K_{\alpha 1}/K_{\alpha 2}$ was fixed at 0.5 and the full-width at half maximum intensity (FWHM) was measured for the main three peaks.

The crystallite size D of the RuO_2 phase can be obtained from the measured FWHM using Scherrer equation [21]:

$$D = \frac{k\lambda}{\beta \cos\theta} \tag{2}$$

where k is a correction factor taken as 0.89, λ is the wavelength of the Cu K_α line ($\lambda = 1.54060$ Å), θ is the Bragg angle of the selected line and $\beta = (B^2 - b^2)^{1/2}$ with B the FWHM and b the resolution parameter of the diffractometer. This last parameter b was measured on silicon, and is equal to 0.0865° at $2\theta = 28.4°$. The uncertainty on the FWHM was considered as 0.002° for the silicon sample and as 0.005° for FNOC57–RuO_2 composites.

A Rietveld refinement was performed using the software FULLPROF® with the WINPLOTR® interface to evaluate the lattice parameters of the main phase. The diffractograms conducted at different temperatures and different amounts of RuO_2 were compared with theoretical diffractograms of RuO_2 established from the structure determined by Takeda et al. [22].

3. Results

3.1. Volatility

In order to estimate the amount of RuO_2 lost by evaporation during a 2-h heat treatment at 1100 °C, several FNOC57–RuO_2 composites were synthesised, with RuO_2 amounts in the range 0–8 wt%. For comparison, samples with 0 and 4 wt% RuO_2 were also synthesised at 1100, 1300, 1400 and 1500 °C. Mass losses of the pure glass frit were of 0.07 ± 0.03% at 1100 °C, of 0.17% at 1300 °C, of 0.52% at 1400 °C and of 1.10% at 1500 °C.

RuO_2 losses obtained at 1100 °C are plotted as a function of the RuO_2 content (2–4 wt%) in Fig. 2(a). Error bars indicated on the graphs correspond to an uncertainty estimated considering only the accuracy of the weighing (±0.002 g). Losses calculated for initial RuO_2 amounts above 2 wt% are all non-significantly different, and give a mean value of 3.1% (with a standard deviation of 0.3%), which fairly agrees with Wilds' values [19] of 2.8–7.5% for a 3-h-thermal treatment at 1150 °C. Below 2 wt%, obtained volatilities move away from this value, probably because of the very low mass of RuO_2 contained in the sample and the increasing uncertainty of possible matter losses. This is why they are not presented in Fig. 2(a).

The temperature dependence of the RuO_2 losses is then shown in Fig. 2(b) for a RuO_2 amount of 4 wt% and temperatures between 1100 and 1500 °C. Fig. 2(b) also presents the volatility measured on pure RuO_2 heated at 900, 1100 and 1300 °C under argon for two hours (at 1300 °C, RuO_2 was reduced to metal). An inert atmosphere was used since heating under air resulted in the complete evaporation of the RuO_2 samples.

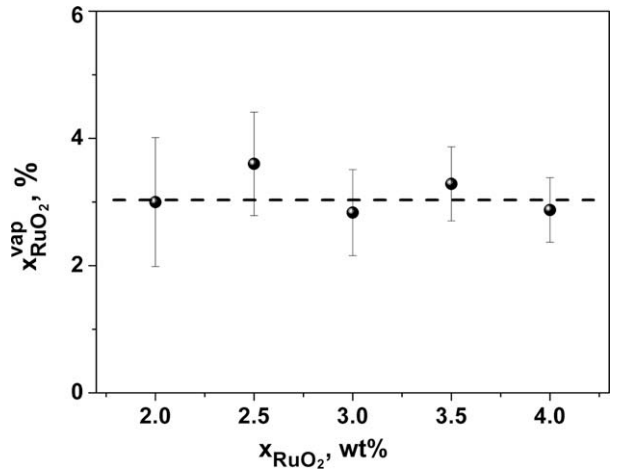

Fig. 2a. Estimation of RuO_2 volatility (as defined in Eq. (1)) by mass losses during melting and 2-h thermal treatment at 1100 °C: 3.1% loss (±0.3).

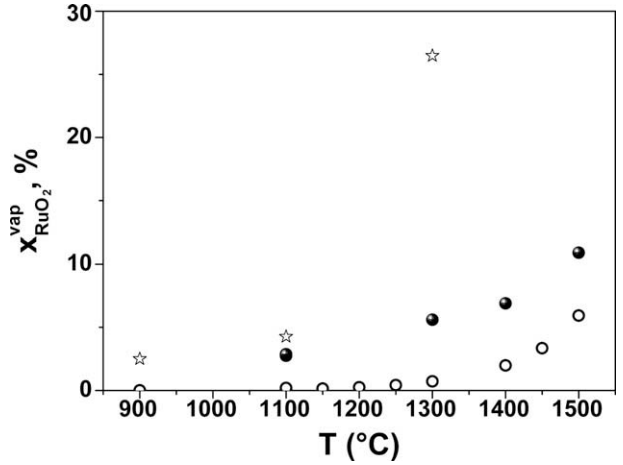

Fig. 2b. Estimation via mass loss measurements of RuO_2 volatility (as defined in Eq. (1)) during a 2-h-heat treatment at T: ● in FNOC57–4RuO_2 under air, ☆ in pure RuO_2 under argon. (○) Comparison with the vapour in thermodynamical equilibrium with RuO_2 as calculated using Factsage™.

Finally, Fig. 2(b) also presents the total amounts of gaseous ruthenium species in thermodynamic equilibrium with RuO_2 calculated using the Factsage™ software. Reagents considered in this calculation are solid RuO_2 and gaseous O_2, with an oxygen activity fixed to 0.9. The amount of all the species (solid and gaseous) in equilibrium with the mixture are then calculated for different temperatures from 800 to 1500 °C by the Factsage™ software [23]. The oxygen activity was fixed to 0.9 because this value is very close to the oxygen activity in oxidised glasses [24].

The obtained RuO_2 volatility at 1100 °C is 3.1 ± 0.3%. It then increases with temperature: 5.6 ± 0.2% at 1300 °C, 6.9 ± 0.2% at 1400 °C and 10.9 ± 0.2% at 1500 °C. The same temperature tendency is observed in the case of pure RuO_2 under argon but with higher values of the volatility than in the presence of the glass matrix. This increase of the volatility with temperature is not surprising: indeed the amount of gaseous ruthenium species in equilibrium with RuO_2, as calculated using Factsage™, also increases with temperature, as can be seen in Fig. 2(b). The experimental volatilities observed here in both systems (pure RuO_2 and RuO_2 in glass) are higher than the calculated equilibrium one because the present system is not closed. The difference between the volatility from RuO_2 in glass and RuO_2 at thermodynamic equilibrium is less marked at 1400–1500 °C. This can be explained by the reduction of RuO_2 through the important evaporation of RuO_3 and RuO_4. The amount of gaseous ruthenium species above the formed metallic Ru is then lower.

3.2. Density

Density measurements are commonly used in order to determine the RuO_2 content in glass–RuO_2 composites in a simple way. Indeed, assuming that no interaction exists between the glass matrix and ruthenium dioxide, the molecular volume of the composite ($V_{composite}$) should be expressed as a linear combination of the molecular volumes of RuO_2 particles (V_{RuO_2}) and of the pure glass frit (V_{glass}):

$$V_{composite} = y_{RuO_2} \times V_{RuO_2} + y_{glass} \times V_{glass}. \quad (3)$$

In this equation, y_{RuO_2} (resp. y_{glass}) is the volume fraction of RuO_2 (resp. of the glass) in the composite. The density of the composite $d_{composite}$ is then expressed as follows, where x_{RuO_2} stands for RuO_2 mass fraction and d_{glass} for the density of the glass matrix free of RuO_2:

$$\frac{1}{d_{composite}} = \frac{x_{RuO_2}}{d_{RuO_2}} + \frac{(1 - x_{RuO_2})}{d_{glass}}. \quad (4)$$

The density of RuO_2 d_{RuO_2} was taken equal to 6.97 g cm^{-3}. Densities were measured for FNOC57–RuO_2 composites with RuO_2 mass fractions in the range 0–8 wt%, all submitted to a 2-h heat treatment at 1100 °C. Fig. 3 shows a comparison of experimental densities (squares) and densities obtained through Eq. (5) (full line), thus assuming that the particles do not interact with the glass matrix. Indicated RuO_2 contents were corrected for volatilisation. Experimental densities show a linear evolution with the RuO_2 content, too, but the slope (1.52 ± 0.06) is lower than in the absence of interactions (1.64). For RuO_2 contents below 1 wt% the difference is negligible; on the contrary in the assumption of the absence of interactions, the density of a 4 wt% RuO_2 composite is overestimated by approximately 0.2% and that of a composite with 8 wt% RuO_2 by approximately 0.7%. In other words, if Eq. (4) is used to estimate the RuO_2 amount in the composite, the latter is underestimated by 5–13%, depending on the RuO_2 amount in the range 0–8 wt%.

3.3. Microscopy observations

Fig. 4(a) and (b) give an example of SEM pictures of a FNOC57–4 wt% RuO_2 sample synthesized at 1200 °C; dark zones correspond to the glass matrix and light grey ones to RuO_2. No continuous chain can be observed. However, it can be seen that RuO_2 particles are not dispersed homogeneously in the glass matrix but tend to agglomerate, building particle-rich zones and zones of pure glass. In Fig. 4(b), ruthenium-rich zones appear to be made up of clusters of RuO_2 nanoparticles (large enough to be detected by SEM analysis) and of RuO_2 grains (probably composed of numerous crystallites) of about 1–5 μm.

Fig. 5(a) and (b) present TEM patterns obtained from a similar sample, but synthesized at 1100 °C. As shown in Fig. 5(a), a similar gathering of RuO_2 particles is observed at the sub-micrometer scale and zones of pure glass can be observed (Fig. 5(b)). Most observable nanoparticles have a 50–100 nm size, and it was checked by electron diffraction that these particles are single-crystals. The TEM analyses performed on various samples of FNOC57–RuO_2 showed only few isolated very small nanoparticles. However, their detection is not easy here. Indeed, due to the signal of the glass matrix, the critical size of a RuO_2 nanoparticle to be detected is not only driven by the resolution of the TEM. Nevertheless, no very small Ru-clusters (though larger than 1 nm) have been observed.

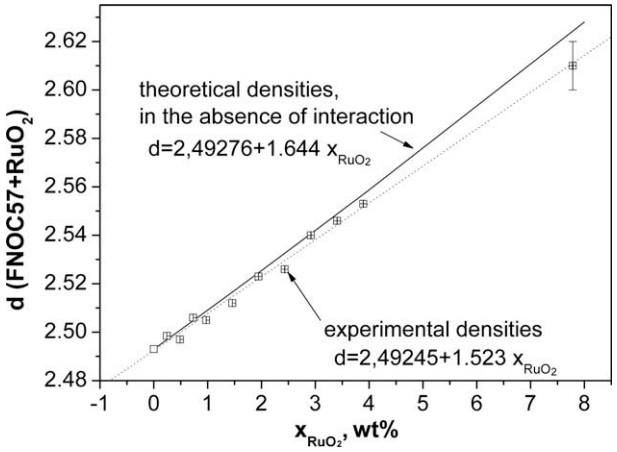

Fig. 3. Comparison of experimental densities (black squares) of glass frit–RuO_2 composites synthesised at 1100 °C with densities estimated for an ideal mixture (full line) assuming the absence of interactions (through Eq. (4)). The uncertainty on the measured density at 8 wt% RuO_2 is larger due to the increasing inhomogeneity of composites at high RuO_2 contents.

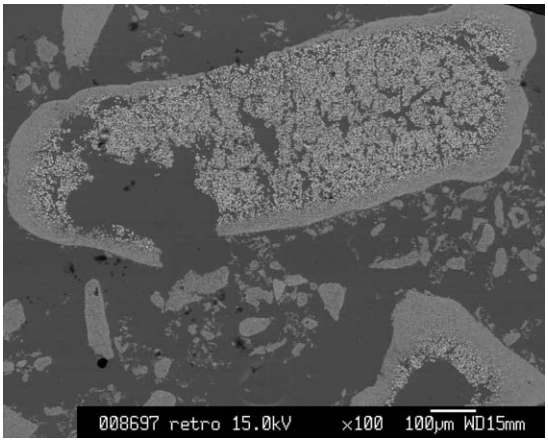

Fig. 4a. SEM pictures of a FNOC57–4 wt% RuO_2 sample synthesized at 1200 °C; dark zones correspond to the glass matrix and light grey ones to RuO_2.

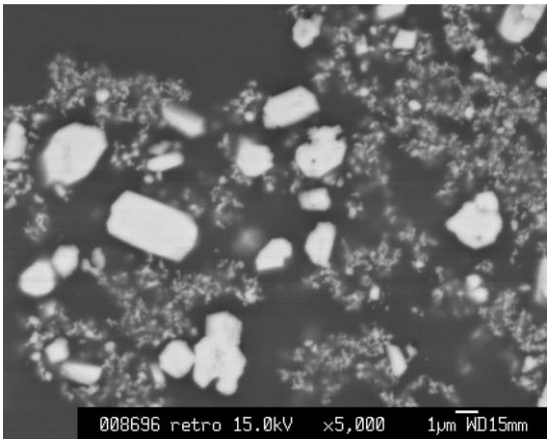

Fig. 4b. Detail of Fig. 4a.

3.4. Crystallite size

3.4.1. Evolution with time of the crystallite size in the glass melt

The main three RuO_2 diffraction peaks, positioned at $2\theta = 28.02°$, $2\theta = 35.07°$ and $2\theta = 54.27°$, are well-defined enough to allow a determination or at least an estimation of the corresponding crystallite sizes. They correspond to the (1 1 0), (1 0 1) and (2 1 1) diffraction planes. The initial sizes of RuO_2 crystallites were measured on raw RuO_2 powder: they are, in the directions perpendicular to these three planes, 10.3 ± 0.3, 11.7 ± 0.3 and 10.0 ± 0.3 nm.

The size evolution with time of RuO_2 crystallites in FNOC57–RuO_2 composites was followed *in situ* during thermal treatments at 800, 1050, 1100 and 1200 °C, via the FWHM of RuO_2 main diffraction peak ($2\theta = 28°$, (1 1 0) diffraction plane). Actually, RuO_2 crystallites are not homogeneous in size (see for instance SEM pictures 4a and 4b); the size thus derived from the FWHM measurement is a crystallite-volume-weighted average size. Therefore, the present work focuses on the crystallite size evolution and not on absolute values. The obtained size evolutions at 800, 1050, 1100 and 1200 °C are shown in Fig. 6. A fast initial increase in size is observed in all cases. However, the final size is obtained after about 40 min at 1200 °C and much faster at 800 °C, whereas the crystallite size slowly increases continuously at 1050 and 1100 °C. Besides, at the end of the scan series, the temperature was quenched in 2–3 min, imitating the glass quenching in the standard synthesis, and the corresponding room temperature crystallite size was then measured (last point in each curve). It remains the same as during the temperature plateau. This validates the measurement of crystallite sizes on quenched samples.

3.4.2. Evolution of the crystallite size with temperature

The size evolution of the crystallites with temperature was followed either *in situ* (at 600, 800, 1050, 1100 and 1200 °C) or at room temperature on quenched samples (synthesized at 1000, 1100, 1200, 1300, 1400 and 1500 °C).

The obtained size evolution versus temperature is presented in Fig. 7 for the (1 1 0) diffraction plane. Similar trends and sizes were obtained for the (1 0 1) and (2 1 1) diffraction planes. Here it has to be specified that sizes at high temperatures (above 1300 °C) must be considered as indicative values only. Indeed, Scherrer equation is valid only for sizes up to approximately 100 nm given the resolution of our laboratory diffractometer. In particular, the FWHM values become very small for bigger crystallites, and the uncertainty on their sizes consequently increases. Nevertheless, the crystallite size is seen to increase greatly with temperature: this increase is already noticeable at 950 °C; it rises up quickly to 1300 °C and then slows down beyond. The final size at 1400 °C is about 10 times bigger than the initial one whatever the diffraction plane considered ((1 1 0), (1 0 1) and (2 1 1)). This corresponds to increases along *a*-, *b*- and *c*-axes of the same order of magnitude (around 10 times between raw RuO_2 powder and crystallites at 1400 °C, which corresponds to a total volume increase of about three orders of

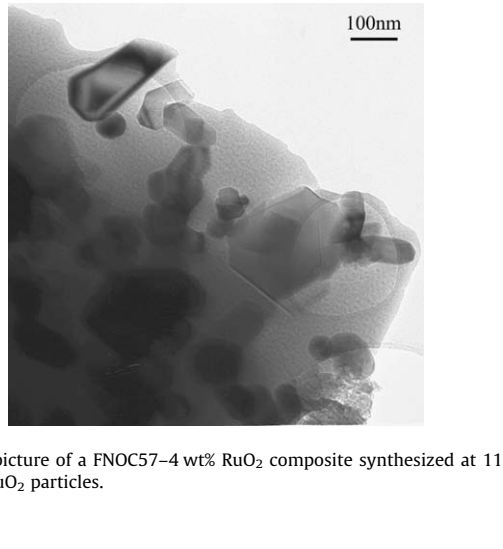

Fig. 5a. TEM picture of a FNOC57–4 wt% RuO_2 composite synthesized at 1100 °C; zone rich in RuO_2 particles.

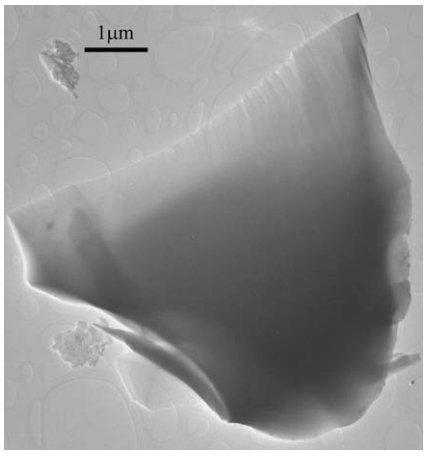

Fig. 5b. TEM picture of a FNOC57–4 wt% RuO_2 composite synthesized at 1100 °C; zone of pure glass.

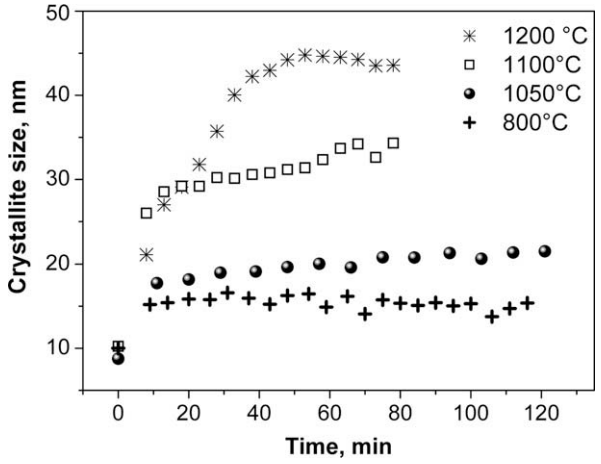

Fig. 6. Evolution of the RuO_2 crystallite size in the (1 1 0) direction vs. time; FNOC57–4 wt% RuO_2 composite; temperatures of 800, 1050, 1100 and 1200 °C.

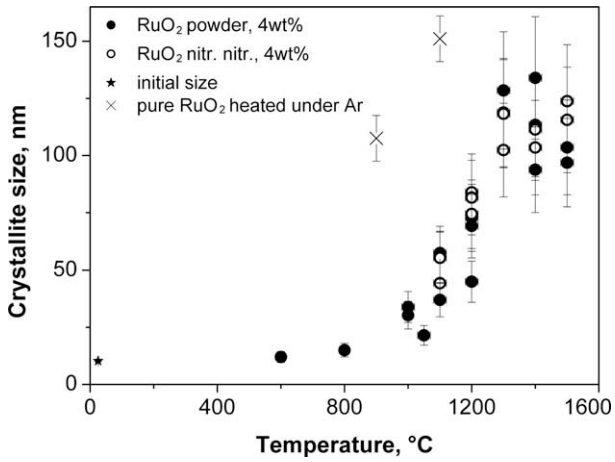

Fig. 7. Evolution with the synthesis temperature of the crystallite size perpendicularly to the (1 1 0) diffraction plane; two RuO_2 precursors were used: RuO_2 powder (●) and a solution of ruthenium nitrosyle nitrate (○). Crystallite sizes obtained in pure RuO_2 heated under argon are also indicated (×).

magnitude). Thus, the initial grain shape seems to be conserved and no tendency to form needles is observed.

When a solution of ruthenium nitrosyle nitrate is used as RuO_2 precursor (white dots in Fig. 7), the same crystallite sizes are obtained as with a powder precursor (black dots in Fig. 7). Thus, the crystallite sizes and shapes appear not to depend on the RuO_2 precursor nature.

Crystallite sizes obtained for pure RuO_2 heated 2 h under argon are also shown in Fig. 7 (crosses): they are of 107 nm at 900 °C and of 151 nm at 1100 °C.

3.4.3. Volume of the cell

A Rietveld refinement was applied to the room temperature diffractograms of FNOC57–RuO_2 composites synthesised at different temperatures in the range of 1000–1400 °C and with different RuO_2 contents, in order to determine the lattice parameters (a and c). The unit cell volume was then calculated and was found not to change with the synthesis temperature and with the amount of RuO_2: 62.660 ± 0.012 Å^3.

4. Discussion

Several indications of the interaction of ruthenium dioxide and the glass matrix FNOC57 have been studied here, in order to progress in the understanding of the observed very low electrical percolation threshold (about 1.5–2.0 wt% RuO_2 i.e. less than 0.7 vol.% [1]).

The ruthenium segregation observed by SEM, leaving entire zones of pure glass (see Fig. 5(b)), can indeed lower the percolation threshold well below the geometrical percolation threshold of 16 vol.% (see for instance the computer simulations of Lebovka et al. [25]). Such a formation of regions rich in RuO_2 particles was also observed by Adachi et al. [2] in lead–borosilicate glasses, though it was considered to be due to the firing process (since obtained regions of pure glass had the size of the initial glass pieces). However, in our case and in Adachi's, the observed RuO_2 chains are not continuous, and moreover a matrix layer is always present between the RuO_2 particles. Therefore, there is the need of electron relays between the particles to explain the electronic conduction. Adachi et al. brought to light an appreciable diffusion of ruthenium in glass, of at least 1 μm after 1 h at 900 °C. Since on the other hand Ru solubility was very limited (up to 200 ppm but below the detection limit for most compositions they studied), they suggested that 'the dissolved Ru ions' were 'taking the form of clusters less than 1 nm size in low-lead glasses'. This hypothesis of the existence of ruthenium nanoclusters was supported by the results of EXAFS studies performed by Sacchi et al. [26], who compared the Fourier transformed signals of RuO_2 in a 67 wt% SiO_2–33 wt% B_2O_3 glass (Ru/glass ≈ 1.5 wt%) heated at 1300 °C for 4 h with pure RuO_2. They observed a similar amplitude for the first peak but a strong reduction in the amplitude of larger interatomic distance peaks, which they explained by the presence of clusters of less than 1 nm.

In the present study, no Ru based-clusters larger than 1 nm were observed during the TEM investigations. Thus, the role of electron relays is probably played by smaller entities, such as physically or chemically dissolved ruthenium, which in fact would correspond to Adachi's clusters [2,3]. All the results presented here are in good agreement with this hypothesis.

First of all, the measured densities of the composites are always found to be lower than the densities calculated in the absence of interactions, and this volume expansion is roughly proportional to the RuO_2 fraction. But this observed volume expansion is not due to changes in the RuO_2 unit cell volume, as was checked by Rietveld analysis. Indeed, the unit cell volume was found not to vary with RuO_2 content and to correspond with its value for pure RuO_2 (within 0.02%, while an increase of up to 35% for 8 wt% RuO_2 would be necessary to account for the density changes). This means that the glass matrix has expanded (by 2% for a RuO_2 content of 4 wt%), either in the vicinity of the RuO_2 particles, because of rearrangements of chemical bonds and of the presence of physically dissolved ruthenium oxides, or in the bulk, also because of the presence of physically dissolved ruthenium oxides.

Another clear indication of the presence of dissolved ruthenium is the growth of RuO_2 crystallites in the glass melt. Indeed, it has been shown here that RuO_2 crystallite size increases with the temperature of the thermal treatment, and the measured kinetics indicate a diffusion-limited growth. Ostwald ripening of RuO_2 particles was also observed by Nakano et al. [7] on borosilicate and on lead glasses, and by Prabhu and Vest [8] on lead–borosilicate glasses.

The Ostwald ripening [7] or the Lifshitz, Slyviziv and Wagner theory (LSW theory) [27] describes the kinetics of growth of particles in a supersaturated solution where the nucleation stage has completed. The decrease of the free energy of the system is then mainly due to a decrease in the total interfacial energy. In this theory, for the diffusion- controlled mechanism the average particle radius r increases with time according to the equation:

$$r^3 - r_0^3 = Kt, \tag{5}$$

where r_0 is the average radius at time $t = 0$, and K is the rate constant depending on the particle matrix interface energy (γ), diffusion coefficient (D), molar volume of particles (V_m), equilibrium saturated concentration (C_∞), gas constant (R) and temperature (T) according to the equation:

$$K = \frac{8\gamma D V_m C_\infty}{9RT}. \tag{6}$$

Fig. 8 shows the time evolution of r^3 obtained from the crystallite sizes measured at 800, 1050, 1100 and 1200 °C. Below 1200 °C this evolution gets linear after a more abrupt start (during the heating of the sample), which suggests a diffusion-limited growth of these crystallites in our system. Moreover, the slope of the linear fits, which represents the rate constant K, increases with the temperature. This result is in agreement with the diffusion-controlled particle growth as described here. Indeed both the diffusion coefficient and the equilibrium saturated concentration increase with temperature. This result indicates that the dissolution of ruthenium oxide into the melt may be a critical factor responsible for the crystallite growth. At 1200 °C, the growth kinetics are faster

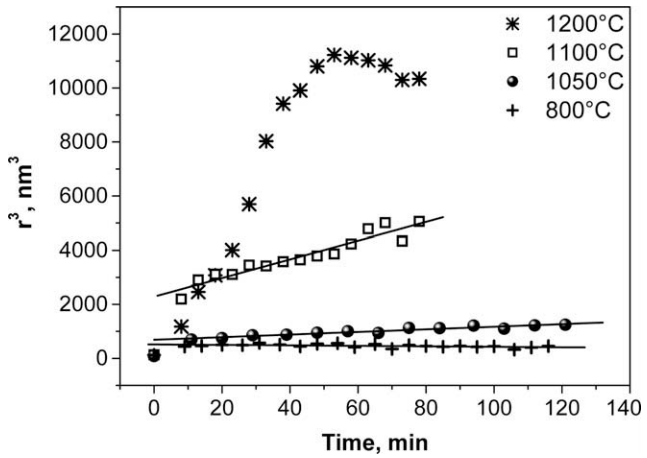

Fig. 8. Time evolution of the crystallite sizes at 800, 950, 1050 and 1100 °C and linear fits.

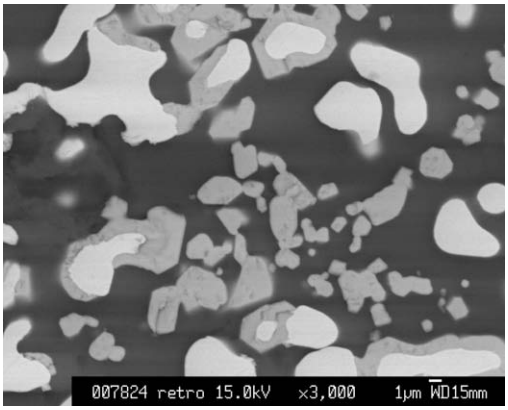

Fig. 10. SEM picture of a FNOC57–4RuO_2 sample submitted to a 2 h-heat treatment at 1500 °C. Black zones correspond to the glass matrix, light grey ones to Ru and dark grey ones to RuO_2.

and not linear any more: this may be explained by a higher ruthenium volatility and a lower viscosity of the melt, which makes convection not negligible any more.

Finally, the interaction of the physically or chemically dissolved ruthenium with the glass matrix is also indicated by the lower crystallite sizes and the lower RuO_2 volatilities obtained in the presence of this matrix. This can be explained by the molten glass matrix restraining the diffusion and the evaporation of ruthenium oxide, its viscosity preventing an easy access of the dissolved ruthenium to the RuO_2 crystallites and to the atmosphere. Support to this explanation was brought by independent volatility measurements on a series of simple borosilicate glasses, the viscosity η of which was made to vary in varying the Na_2O content in order to study the influence of the diffusion coefficient D on the volatilisation. According to the fundamental Stokes–Einstein equation, for a given temperature the diffusion coefficient D of a Brownian particle of radius r is inversely proportional to the shear viscosity η:

$$D = \frac{kT}{6\pi\eta r} \tag{7}$$

Measured volatilities for a 2-h heat treatment at 1200 °C are plotted in Fig. 9 vs. the reciprocal viscosity at 1200 °C (viscosity values taken from [28]). The obtained correlation is linear meaning

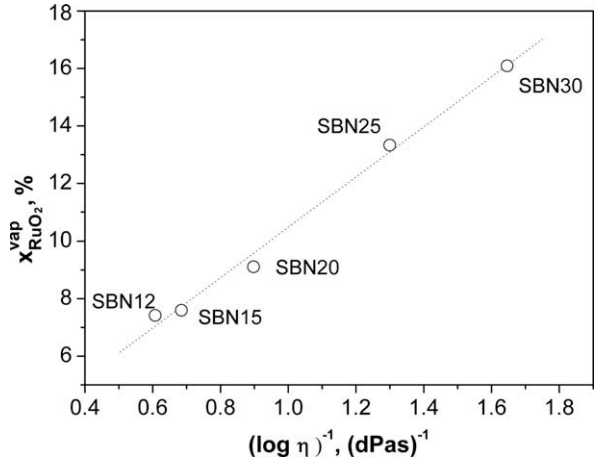

Fig. 9. Volatility vs. the reciprocal viscosity for a series of sodo-borosilicate glasses with various Na_2O contents (the volatility was measured from mass losses after 2 h at 1200 °C and viscosity values are those given at 1200 °C by Grandjean et al. in [28]).

that the volatility is proportional to the diffusion coefficient and that RuO_2 volatility is indeed restrained by ruthenium species diffusion in the melt.

Ruthenium oxide physical and chemical dissolution leads to losses by volatility, but also, through reprecipitation, to the growth of RuO_2 crystallites. It may also be responsible for another observed feature: though most particles observed in SEM investigations after a thermal treatment at relatively high temperature (1400–1500 °C) are made of pure RuO_2 or pure Ru, some of them present a particular structure of a Ru core covered by a RuO_2 shell (see Fig. 10). This shell may have been formed by reprecipitation of dissolved ruthenium species on already formed particles during cooling.

5. Conclusion

A series of RuO_2–borosilicate glass composites was studied, with RuO_2 amounts of the order of what is observed in vitrified nuclear waste. The amount of RuO_2 lost by evaporation during a 2-h thermal treatment at 1100 °C was measured to be 3 wt% of the initial RuO_2 mass, and to increase with temperature. Besides, it was shown that the amount of volatilised ruthenium at a given temperature increases linearly vs. the reciprocal viscosity of the glass melt, indicating that the volatility is restrained by the glass melt viscosity.

In the quenched glass the remaining ruthenium is mostly in the form of RuO_2 grains and was shown to induce an expansion of the matrix volume, indicating a modification of the glass structure, possibly due to the presence of chemically or physically dissolved ruthenium. It would be interesting to study in details this modification of the glass structure in the presence of ruthenium, e.g., using spectroscopy investigations (Raman, NMR). Another clear indication of the presence of this dissolved ruthenium in the glass melt, namely Adachi's ruthenium nanoclusters [2], is the growth of RuO_2 crystallites, the kinetics of which appears to be diffusion-limited.

Acknowledgments

The authors wish to thank Pierre Pérouty (CEA Valrhô, Bagnols-sur-Cèze, France) for the SEM analyses, Marie-Louise Saboungi, director of the CRMD (Orleans, France), for the TEM access, and Damien Hudry (CEA Valrhô, Bagnols-sur-Cèze, France) for fruitful discussions on the analysis of X-ray diffraction spectra.

References

[1] R. Pflieger, M. Malki, Y. Guari, J. Larionova, A. Grandjean, J. Am. Ceram. Soc., accepted for publication.
[2] K. Adachi, S. Iida, K. Hayashi, J. Mater. Res. 9 (7) (1994) 1866.
[3] K. Adachi, H. Kuno, J. Am. Ceram. Soc. 83 (10) (2000) 2441.
[4] H.D. Schreiber, F.A. Settle Jr., P. Lynne Jamison, J.P. Eckenrode, G.W. Headley, J. Less Common Met. 115 (1986) 145.
[5] J. Mukerji, S.R. Biswas, Glass Ceram. Bull. 14 (1967) 30.
[6] C. Simonnet, A. Grandjean, J. Phalippou, J. Nucl. Mater. 336 (2005) 243.
[7] T. Nakano, K. Suzuki, T. Yamaguchi, J. Adhes. 46 (1994) 131.
[8] A.N. Prabhu, R.W. Vest, Mater. Sci. Res. 10 (1975) 399.
[9] C. Simonnet, A. Grandjean, J. Non-Cryst. Solids 351 (2005) 1611.
[10] P.J.S. Ewen, J.M. Roberston, J. Phys. D: Appl. Phys. 14 (1981) 2253.
[11] A. Kusy, Physica B 240 (1997) 226.
[12] G.E. Pike, C.H. Seager, J. Appl. Phys. 48 (1977) 5152.
[13] C. Krause, B. Luckscheiter, J. Mater. Res. 6 (12) (1991) 2535.
[14] T. Sato, J. Radioanal. Nucl. Chem. Art. 129 (1) (1989) 77.
[15] Z. Hölgye, J. Radioanal. Nucl. Chem. Lett. 117 (6) (1987) 353.
[16] C. Mun, L. Cantrel, C. Madic, Nucl. Technol. 156 (2006) 332.
[17] U. Backman, M. Lipponen, A. Auvinen, U. Tapper, R. Zilliacus, J.K. Jokiniemi, Radiochim. Acta 93 (2005) 297.
[18] H. Kamizono, S. Kikkawa, Y. Togashi, S. Tashiro, J. Am. Ceram. Soc. 72 (8) (1989) 1438.
[19] G.W. Wilds, Report DP-MS-78-13, CONF-780819-26, in: 15th Nuclear Air Cleaning Conference, August 1978, Boston, MA, USA, January 1978.
[20] A. Grandjean, M. Malki, C. Simonnet, J. Non-Cryst. Solids 352 (2006) 2731.
[21] R. Jenkins, R.L. Snyder, X-ray Powder Diffractometry, Wiley-Interscience, 1996. p. 89.
[22] T. Takeda, M. Nagata, H. Kobayashi, R. Kanno, Y. Kawamoto, M. Takano, T. Kamiyama, F. Izumi, A.W. Sleight, J. Solid State Chem. 140 (1998) 182.
[23] C.W. Bale, P. Chartrand, S.A. Decterov, G. Eriksson, K. Hack, R. Ben Mahfoud, J. Melançon, A.D. Pelton, S. Petersen, Calphad J. 62 (2002) 189.
[24] O. Pinet, unpublished results.
[25] N. Lebovka, M. Lisunova, P. Mamunya Ye, N. Vygornitskii, J. Phys. D: Appl. Phys. 39 (2006) 2264.
[26] M. Sacchi, M. Antonini, M. Prudenziati, Phys. Status Solidi A 109 (1988) K23.
[27] O.N. Senkov, Scr. Mater. 59 (2008) 171.
[28] A. Grandjean, M. Malki, C. Simonnet, D. Manara, B. Pénelon, Phys. Rev. B 75 (2007) 054112.